Published in final edited form as:
Int J Parasitol. 2009 October ; 39(12): 1331–1344. doi:10.1016/j.ijpara.2009.06.002.

Glycotope analysis in miracidia and primary sporocysts of *Schistosoma mansoni*: Differential expression during the miracidium-to-sporocyst transformation

Nathan A. Peterson[a], **Cornelis H. Hokke**[b], **André M. Deelder**[b], and **Timothy P. Yoshino**[a,*]

[a]Department of Pathobiological Sciences, University of Wisconsin – Madison, School of Veterinary Medicine, 2115 Observatory Drive, Madison, WI 53706, USA [b]Department of Parasitology, Center for Infectious Diseases, Leiden University Medical Center, Albinusdreef 2, 2333 ZA Leiden, The Netherlands

Abstract

Fucosylated carbohydrate epitopes (glycotopes) expressed by larval and adult schistosomes are thought to modulate the host immune response and possibly mediate parasite evasion in intermediate and definitive hosts. While previous studies showed glycotope expression is developmentally and stage-specifically regulated, relatively little is known regarding their occurrence in miracidia and primary sporocysts. In this study, previously defined monoclonal antibodies were used in confocal laser scanning microscopy, standard epifluorescence microscopy and Western blot analyses to investigate the developmental expression of the following glycotopes in miracidia and primary sporocysts of *Schistosoma mansoni*: GalNAcβ1-4GlcNAc (LDN), GalNAcβ1-4(Fucα1-3)GlcNAc (LDN-F), Fucα1-3GalNAcβ1-4GlcNAc (F-LDN), Fucα1-3GalNAcβ1-4(Fucα1-3)GlcNAc (F-LDN-F), GalNAcβ1-4(Fucα1-2Fucα1-3)GlcNAc (LDNDF), Fucα1-2Fucα1-3GalNAcβ1-4(Fucα1-2Fucα1-3)GlcNAc (DF-LDN-DF), Galβ1-4(Fucα1-3)GlcNAc (Lewis X) and the truncated trimannosyl N-glycan Manα1-3(Manα1-6)Manβ1-4GlcNAcβ1-4GlcNAcβ1- Asn (TriMan). All but Lewis X were variously expressed by miracidia and sporocysts of *S. mansoni*. Most notably, α3-fucosylated LDN (F-LDN, F-LDN-F, LDN-F) was prominently expressed on the larval surface and amongst glycoproteins released during larval transformation and early sporocyst development, possibly implying a role for these glycotopes in snail–schistosome interactions. Interestingly, Fucα2Fucα3- subsituted LDN (LDN-DF, DF-LDN-DF) and LDN-F were heterogeneously surface-expressed on individuals of a given larval population, particularly amongst miracidia. In contrast, LDN and TriMan primarily localised in internal somatic tissues and exhibited only minor surface expression. Immunoblots indicate that glycotopes occur on overlapping but distinct protein sets in both larval stages, further demonstrating the underlying complexity of schistosome glycosylation. Additionally, sharing of specific larval glycotopes with *Biomphalaria glabrata* suggests an evolutionary convergence of carbohydrate expression between schistosomes and their snail host.

Keywords

Schistosoma mansoni; *Biomphalaria glabrata*; Miracidium; Sporocyst; Transformation; Carbohydrate; Parasite–host interaction; Monoclonal antibody

*Corresponding author. Tel.: +1 608 263 6002; fax: +1 608 262 7871. yoshinot@svm.vetmed.wisc.edu (T.P. Yoshino).

1. Introduction

Parasitic flatworms of the genus *Schistosoma* infect an estimated 200 million people, with over 770 million at risk, in 74 countries worldwide (Chitsulo et al., 2000; Steinmann et al., 2006). Chronic human schistosomiasis results from granulomatous inflammation in response to parasite eggs that accumulate in host tissues (Ross et al., 2002). Surface-expressed and secreted carbohydrates (CHOs) are key determinants that drive this pathogenesis, with oligosaccharide elements playing roles in egg sequestration, Th2 immune biasing, granuloma formation and strong antibody responses in human hosts (Jacobs et al., 1999a, b; Lejoly-Boisseau et al., 1999; Eberl et al., 2001; Nyame et al., 2003; Van De Vijver et al., 2004, 2006).

Schistosome glycoconjugates present a variety of immunologically important terminal CHO structures (herein referred to as “glycotopes“), including GalNAcβ1-4GlcNAc (LDN), GalNAcβ1- 4(Fucα1-3)GlcNAc (LDN-F), Fucα1-3GalNAcβ1-4GlcNAc (F-LDN), Fucα1-3GalNAcβ1-4(Fucα1-3)GlcNAc (F-LDN-F), GalNAcβ1-4 (Fucα1-2Fucα1-3)GlcNAc (LDN-DF), Fucα1-2Fucα1-3GalNAcβ1-4(Fucα1-2Fucα1-3)GlcNAc (DF-LDN-DF), Galβ1-4(Fucα1-3)GlcNAc (Lewis X) and the truncated trimannosyl N-glycan Manα1- 3(Manα1-6)Manβ1-4GlcNAcβ1-4GlcNAcβ1-Asn (herein termed “TriMan”) (Table 1) (van Remoortere et al., 2000, 2003; Wuhrer et al., 2002; Nyame et al., 2003; Robijn et al., 2005; van Roon et al., 2005; Lehr et al., 2008). These and other glycotopes have been variously observed as conjugates of proteins and lipids in most stages of the schistosome life cycle, particularly the mammalian host-associated stages, and their expression appears to be developmentally and in some cases gender-specifically regulated (van Remoortere et al., 2000; Robijn et al., 2005; Wuhrer et al., 2006).

Parasite-associated glycotopes have been clearly implicated in human schistosomiasis, but their role in snail infections is much less understood. Previous studies have demonstrated that snail hemocytes (immune effector cells) express CHO-binding proteins, or lectins, which may function as surface receptors and/or secreted opsonins that mediate cytotoxic killing of parasite larvae (Castillo et al., 2007; Yoshino et al., 2008). Additionally, while some data indicate that monosaccharide-conjugated neoglycoproteins, including galactosyl- and fucosyl-BSA, are sufficient to elicit cytotoxic reactive oxygen species (ROS) production (Hahn et al., 2000), others suggest a more suppressive role in hemocyte immune function (Plows et al., 2004, 2005). Although these observations predict a role for CHOs in snail–schistosome interactions, the relevance of monosaccharide-driven responses is arguable. In fact, schistosome glycoconjugates generally comprise oligosaccharides having distinct compositions and configurations, which may drive more sophisticated CHO-dependent responses than have been previously demonstrated.

Until recently, the glycotopes expressed in miracidia and sporocysts were largely unknown. Using a mass spectrometry approach for glycomic profiling in *Schistosoma mansoni*, Hokke et al. (2007) showed the occurrence of putatively multifucosylated, LDN-terminating di- and triantennary structures, as well as the presence of the TriMan glycotope, amongst miracidial N-glycans. Lehr et al. (2008) demonstrated the surface expression of F-LDN, F-LDN-F, LDN-F and LDN-DF in miracidia and the presence of these and other (non-fucosylated LDN and Lewis X) glycotopes in secondary sporocysts of *S. mansoni*. Additionally, LDN and LDN-F have been demonstrated in protein extracts of primary sporocysts (Nyame et al., 2002). While these studies provide fundamental information regarding glycosylation in larval schistosomes, they do not adequately describe glycotope expression during larval transformation and subsequent development. Importantly, larvae are most vulnerable to the snail immune response during the miracidium- to-primary sporocyst transformation when miracidia shed their ciliated epidermal plates and form a syncytial tegument (Pan, 1996).

Moreover, the miracidial glycocalyx, which comprises mainly CHOs, is largely lost with the epidermal plates (Chiang and Caulfield, 1988), providing an opportunity for a rapid change in the larval surface coat that may influence the outcome of infection. Clearly a more detailed investigation of glycotope expression in miracidia and primary sporocysts is warranted.

In the present study, previously defined and well-characterised glycotope-specific monoclonal antibodies (mAbs) were used in confocal laser scanning microscopy (CLSM), standard epifluorescence microscopy (EFM) and Western blot analyses to investigate the expression and localisation of schistosome-associated CHO structures in miracidia and in vitro-cultivated primary sporocysts of *S. mansoni*. Additionally, immunoblot analyses were used to examine glycotope expression in epidermal plates and parasite culture supernatants containing larval transformation proteins (LTPs; Wu et al., 2009), both of which are released during transformation and subsequent larval development. As an adjunct to experiments in schistosomes, we also examined *Biomphalaria glabrata* hemocyte and plasma proteins for anti-glycotope antibody reactivity, the results of which provide insights regarding snail–schistosome interactions.

2. Materials and methods

2.1. Isolation and cultivation of S. mansoni larvae

Research protocols involving mice, including routine maintenance and care, used in the course of this study were reviewed and approved by the Institutional Animal Care and Use Committee (IACUC) at the University of Wisconsin – Madison under Assurance No. A3368-01.

Miracidia of *S. mansoni* (NMRI strain) were isolated from infected mouse livers and axenically cultivated as described by Yoshino and Laursen (1995). Briefly, infected mice were sacrificed 7–8 weeks post-exposure to *S. mansoni* cercariae, and livers were excised and homogenised to release the trapped schistosome eggs. Eggs were transferred to artificial pond water to induce hatching (Nolan and Carriker, 1946), and miracidia were collected for immediate use in experiments or for cultivation in Chernin's Balanced Salt Solution (CBSS; Chernin, 1963) containing glucose and trehalose (1 g/L each) as well as penicillin and streptomycin (CBSS+). After 24 h in culture, most miracidia transformed to primary sporocysts, shedding their epidermal plates and forming a syncytial tegument. In this study, parasite cultures were maintained in CBSS+ for 2 and 8 days before experimentation. Additionally, primary sporocysts were kept for 21 days in conditioned complete *B. glabrata* embryonic (Bge) cell medium (ccBge) prepared from culture supernatants of 4-day maintained Bge cells as previously described (Yoshino and Laursen, 1995; Vermeire et al., 2004). In both parasite cultures, the medium was changed every 3–4 days.

2.2. Anti-glycotope mAbs

This investigation utilised a panel of previously defined carbohydrate- specific mAbs that recognise schistosome-associated fucosylated and non-fucosylated terminal glycan epitopes (glycotopes). Antibody specificities and pertinent literature references are summarised in Table 1.

2.3. Processing of schistosome larvae for fluorescence microscopy

Miracidia and 2-, 8- and 21-day in vitro-cultivated primary sporocysts were washed five times with snail PBS (sPBS: 8.41 mM Na_2HPO_4/1.65 mM NaH_2PO_4~H_2O/45.34 mM NaCl, pH 7.4) and transferred to a Sigmacote®-treated (Sigma–Aldrich, St. Louis, MO, USA) 1.5-mL microfuge tube (Fisher Scientific, Pittsburgh, PA, USA). All in-tube washes and

treatments were performed at 4 °C while rotating, and between incubations parasite larvae were pelleted by centrifugation for 2 min at 300*g*. Larvae were simultaneously fixed and permeabilised by overnight incubation in 2% paraformaldehyde/1% Triton X-100 (Sigma–Aldrich)/sPBS (pH 7.2), washed two times with sPBS and four times with 1% BSA/sPBS (10 min/wash) and blocked overnight with 5% BSA/0.02% azide/sPBS (blocking buffer). Blocked larvae were distributed to Sigmacote®- treated 1.5-mL microfuge tubes (~2000 larvae/tube) and incubated for 5 days in anti-glycotope hybridoma culture supernatants diluted 1/10 in blocking buffer. Secondary antibody-only control larvae were incubated for 5 days in blocking buffer alone. Following primary mAb treatment, larvae were washed five times with 1% BSA/sPBS (10 min/wash) and treated overnight with a solution containing 50 μg/mL Hoechst 33258 dye (Invitrogen, Eugene, OR, USA), 7.5 U/mL Alexa Fluor®546-conjugated phalloidin (Invitrogen) and 4 μg/mL Alexa Fluor®488-conjugated goat anti-mouse secondary antibody (Invitrogen) in blocking buffer. Finally, larvae were washed five times with 1% BSA/sPBS (10 min/wash) and mounted in Vectashield ® mounting medium (Vector Laboratories, Burlingame, CA, USA) on a 24 × 50 mm^2 cover glass (Fisher Scientific). Preparations were then covered with a 22 × 22 mm^2 cover glass (Fisher Scientific) and sealed with nail polish to prevent desiccation. Confocal laser scanning microscopy images were sequentially collected at 600×total magnification under oil immersion using a Radiance 2100 MP Rainbow confocal/multiphoton system (Bio-Rad Laboratories, Hercules, CA, USA) incorporating continuous-wave laser lines of 488 nm and 543 nm for the excitation of Alexa Fluor®488 and 546, respectively, and a diode-pumped femtosecond titanium:sapphire laser tuned to 750 nm for the excitation of Hoechst 33258 dye. Images were processed using LaserSharp v6.0, Adobe Photoshop CS v9.0 and ImageJ v1.37 software, and antibody reactivities were assessed against the secondary antibody-only control and against treatment with anti-LewisXmAb128-4F9-A, which yielded no reactivity relative to the secondary antibody-only control and therefore served as an antibody specificity control (negative control). Furthermore, determination of glycotope localisation was based on descriptions by Schutte (1974), Pan (1980) and Bahia et al. (2006).

Processing of non-permeabilised miracidia and 2-day primary sporocysts was identical to the above protocol with the exception that larvae were fixed in 2% paraformaldehyde/sPBS in the absence of Triton X-100 detergent. Immunostained non-permeabilised larvae were examined by standard EFM using a Nikon Eclipse TE300 inverted microscope (Nikon Instruments, Inc., Melville, NY, USA), and images were collected and processed using MetaMorph v7.0 and Adobe Photoshop CS v9.0 software. Again, mAb binding was assessed against secondary antibody-only control and anti-Lewis X reactivities.

2.4. Isolation and extraction of ciliated epidermal plates

After 18 h of cultivation, parasite larvae and free epidermal plates were suspended and allowed to settle for 4 min, and the plate-enriched culture supernatants were combined and transferred to a 15-mL tube on ice. Again, larvae were allowed to settle out of suspension for 4 min before transferring the supernatant (minus the bottom ~400 μL) to a new tube on ice. Following transfer, the suspension was visually inspected for contaminating larvae. The supernatant was repeatedly settled and transferred seven times, yielding a plate-enriched suspension devoid of larvae. Plates were pelleted by centrifugation at 300*g* and 4 °C for 15 min and suspended in gentle lysis buffer (GLB: 1% octyl-β-D-glucopyranoside (Sigma–Aldrich)/0.5% Triton X-100/sPBS) containing a cocktail of protease inhibitors (CalBiochem, San Diego, CA, USA). Lysis continued on ice for 30 min, after which plate debris was removed by centrifugation at 10,000*g* for 2 min, and the protein content of the lysate was quantified by the bicinchoninic acid (BCA) assay (Pierce, Rockford, IL, USA).

2.5. Collection of parasite culture supernatants containing larval transformation proteins (LTPs)

Parasite culture supernatants containing LTPs, including proteins that are actively excreted and/or secreted by the viable larvae as well as those released by the degradation of shed epidermal plates (Wu et al., 2009), were collected after 2 days in culture. Supernatants were sterilised with a 0.2 μm syringe filter (Nalgene Labware, Rochester, NY, USA) and concentrated ~20-fold with a 3 kDa MWCO centrifugal concentrator (Millipore, Billerica, MA, USA). The protein was then quantified by BCA protein assay according to the manufacturer's recommendations and protein fractions were stored at −80 °C.

2.6. Preparation of whole-body larval extracts

Miracidia and primary sporocysts at 2 and 8 days of cultivation were isolated as above. In a 1.5-mL microfuge tube, larvae were resuspended with ~25 μL of GLB containing protease inhibitors and manually disrupted with a pestle. Parasite homogenates were then diluted to ~600 μL with lysis buffer and vortexed for 5 min. Particulate debris was removed by centrifugation at 10,000*g* for 2 min, and the protein content of the lysate was determined by BCA protein assay according to the manufacturer's recommendations.

2.7. One-dimensional (1D) SDS–PAGE and Western blot analysis of parasite proteins

Whole-body larval extracts, epidermal plate proteins and concentrated culture supernatants containing LTPs were examined by 1D SDS–PAGE and immunoblot analysis as outlined in Sambrook et al. (1989). Samples (3 μg protein/lane) were fractionated on 12.5% polyacrylamide gels and transferred to 0.2 μm nitrocellulose membranes (Bio-Rad Laboratories). Following transfer, gels were stained using a Silver Quest™ silver staining kit (Invitrogen) as outlined by the manufacturer. Membranes were blocked overnight at 4 °C with 5% BSA in tris-buffered saline (TBS: 20 mM Tris/150 mM NaCl, pH 7.5), and lanes were separated by razorblade to be treated individually with anti-glycotope hybridoma culture supernatants diluted 1/100 with 5% BSA/TBS. Membrane strips were incubated with primary antibody overnight at 4 °C on a rocker. Blots were then washed three times (5 min/wash) with TBS containing 0.03% Tween® 20 (Fisher Scientific) (TBST), rinsed in 5% BSA/TBS and treated for 1 h at 22 °C with alkaline phosphatase-conjugated secondary antibody (CalBiochem) diluted 1/5000 with 5% BSA/TBS. Finally, blots were washed three times with TBST (5 min/wash), rinsed with TBS and developed in alkaline phosphatase buffer (100 mM Tris/100 mM NaCl/50 mM $MgCl_2$, pH 9.5) containing 5-bromo-4-chloro-3′-indoylphosphate *p*-toluidine salt and nitro-blue tetrazolium chloride (Pierce) prepared according to the manufacturer's recommendations.

2.8. Extraction of superficially localised larval proteins

Unless indicated otherwise, washes and treatments included intervening centrifugation at 200*g* for 2 min. Live miracidia and in vitro-cultivated primary sporocysts were transferred to 1.5-mL siliconised tubes and washed four times with cold sPBS (pH 7.4). During the final wash, larvae were checked for viability by visual assessment of motility, tegument integrity and/or flame cell activity. Proteins were extracted by incubation for 40 min rotating in GLB (favoring extraction of superficially localised/surface proteins) containing protease inhibitors. Following extraction, parasites were visually assessed for general intactness. Parasite bodies were pelleted by centrifugation at 4500*g* for 5 min, and the protein content of the resultant extract was quantified by BCA assay according to the manufacturer's recommendations. Extracts were distributed into 50 μg aliquots, and aliquots were stored at −80 °C until used.

2.9. Two-dimensional (2D) SDS–PAGE and Western blot analysis of surface-enriched protein extracts

Two-dimensional SDS–PAGE was performed following the recommendations by Berkelman and Stenstedt (1998). Protein aliquots were thawed on ice, and 4 volumes of cold acetone were added. After 20 min on ice, proteins were pelleted by centrifugation for 20 min at 16,000*g* and 4 °C. The pellet was then washed with 1 mL cold acetone and centrifuged for 5 min at 16,000*g* and 4 °C. After removal of the supernatant, the pellet was air-dried and solubilised in 200 μL DeStreak Rehydration Solution containing 0.5% immobilised pH gradient (IPG) buffer (pH 3–10) (GE Healthcare, Piscataway, NJ, USA) and 20 mM DTT (Amersham Bio-sciences, Piscataway, NJ, USA). For each protein aliquot, an 11 cm Immobiline™ DryStrip (pH 3–10, GE Healthcare) was rehydrated for 12 h at 20 °C in the constituted rehydration buffer, and proteins were isoelectricaly focused on an Ettan™ IPGphor IEF platform (GE Healthcare) at 50 μA/dry-strip for 14,000 total Vh: 500 V to 500 Vh, 1000 V to 1000 Vh and 8000 V to 12,500 Vh, with all phases in "step and hold" mode. Immobilised pH gradient strips were then prepared for 2D PAGE-fractionation by a 20 min incubation in SDS-equilibration buffer (2% SDS/50 mM Tris–HCl (pH 8.8)/6 M urea/30% glycerol/0.002% bromophenol blue) containing 65 mM DTT followed by a 20 min incubation in SDS-equilibration buffer containing 135 mM iodoacetamide (Sigma–Aldrich). Each IPG strip was loaded onto a 12.5% polyacrylamide gel and fractionated using a Hoefer SE 600 vertical electrophoresis system (Hoefer, San Fransisco, CA, USA) at 30 mA until completion. Fractionated proteins were then transferred overnight at 30 mA to a 0.2 μm polyvinylidene difluoride membrane using a Trans-Blot Cell transfer system (Bio-Rad Laboratories), and membranes were blocked overnight at 4 °C in 5% BSA/TBS. Membranes were treated overnight at 4 °C with anti-glycotope hybridoma culture supernatants diluted 1/100 with 5% BSA/TBS, washed three times (10 min/wash) with TBST, rinsed with 5% BSA/TBS and incubated away from light for 1 h at 22 °C with Alexa Fluor®680-conjugated goat anti-mouse secondary antibody (Invitrogen) diluted 1/5000 in 5% BSA/TBS. Blots were then washed three times (10 min/wash) with TBST, rinsed with water and allowed to dry. Finally, membranes were scanned using the Odyssey infrared imaging system (LI-COR Biosciences, Lincoln, NE, USA).

2.10. Snail cultivation and preparation of hemocytes and plasma Western blot analysis

Biomphalaria glabrata (BS90 strain) were maintained in dechlorinated artificial pond water at 26 °C on a 12 h:12 h light-dark cycle and fed green leaf lettuce ad libitum. The shells of snails (diameter >10 mm) were swabbed clean with 70% ETOH and air-dried. Hemolymph was obtained by headfoot retraction (Sminia and Barendsen, 1980), pooled in a petri dish on ice, transferred to a 15-mL centrifuge tube and diluted 1:1 with anti-clump buffer (10 mM EDTA/50 mM sodium citrate/25 mM sucrose/TBS, pH 7.4). Hemocytes were pelleted by centrifugation at 200*g* and 4 °C for 5 min, and the diluted plasma (supernatant) was transferred to a 100 kDa MWCO centrifugal filter (Millipore). Hemocytes were washed three times in sPBS, with intervening centrifugations at 200*g* and 4 °C (5 min/spin), and cells were transferred to a 1.5-mL tube on ice. Mean-while, the plasma fraction was centrifuged at 3200*g* and 4 °C in the centrifugal filter, and the flow-through was transferred to a 9 kDa MWCO centrifugal concentrator (Pierce) and concentrated ~18-fold by centrifugation at 3200*g* and 4 °C. The retained protein solution was transferred to a 1.5-mL tube, and protease inhibitors (CalBiochem) were added. Hemocytes and concentrated plasma proteins were suspended in SDS reducing buffer (Novagen, Gibbstown, NJ, USA) and boiled for 10 min, and protein samples were evenly distributed to lanes of a 12.5% polyacrylamide gel to be electrophoretically fractionated and immunoblotted as described above.

3. Results

3.1. Glycotope expression in miracidia and primary sporocysts by fluorescence microscopy

Anti-glycotope mAbs (summarised in Table 1) were used in CLSM and EFM to examine the overall expression and surface localisation, respectively, of glycotopes in miracidia and primary sporocysts of *S. mansoni*. All glycotopes, with the exception of Lewis X, were variously expressed during larval transformation and early primary sporocyst development, with fucosylated derivatives of LDN being prominently, but selectively, displayed at the larval surface and/or in somatic tissues. Moreover, data indicate substantial heterogeneity within a given larval population, particularly amongst miracidia, regarding the expression of certain glycotopes.

Compared to negative controls (Figs. 1A, B and 2A, B; Supplementary Fig. S1A and B), non-fucosylated LDN was broadly distributed within the bodies of both miracidia and primary sporocysts (Fig. 1C and D; Supplementary Fig. S1C and D). Confocal laser scanning microscopy demonstrated its expression in various miracidial organs/structures, including the apical gland, neural mass, interstitial cells and interepidermal ridge cytons. Non-fucosylated LDN also localised within the terebratorium and in a superficial layer just outside the circular and longitudinal muscles. While EFM supports LDN expression in the terebratorium, data indicate that superficial reactivity is not attributable to the ciliated epidermal plates. Instead, LDN was generally expressed in the miracidial interepidermal ridges (Fig. 2C). Despite the sporocyst tegument deriving from these ridges (Samuelson and Caulfield, 1985; Dunn and Yoshino, 1988; Pan, 1996), LDN was not observed by CLSM or EFM on the tegument of primary sporocysts (Fig. 2D).

In contrast to LDN, its α3-fucosylated derivatives, including F-LDN, F-LDN-F and LDN-F, generally localised to the ciliated epidermal plates and interepidermal ridges of miracidia and to the tegument of primary sporocysts (Figs. 1E–J and 2E–J; Supplementary Fig. S1E–J). However, while the surface presentation of F-LDN and F-LDN-F did not vary amongst individual miracidia in EFM preparations, LDN-F exhibited heterogeneous localisation within the larval population. For example, nearly a third of the miracidia featured LDN-F on one or more epidermal plates, with few individuals having all immunopositive plates and fewer still exhibiting localisation in plate-associated cilia. Expression in others was restricted to the interepidermal ridges and terebratorium, while the remaining miracidia lacked surface-expressed LDN-F altogether (Supplementary Fig. S2A–D). By contrast, no heterogeneous surface localisation was observed within the primary sporocyst population. F-LDN, F-LDN-F and LDN-F were also localised in miracidial and sporocyst somatic tissues, including the interstitial cells and interepidermal ridge cytons/matrices (Fig. 1E–J; Supplementary Fig. S1E–J), however internal immunoreactivity varied amongst individuals of both larval stages.

Glycotopes LDN-DF and DF-LDN-DF, the α2-fucosylation products of LDN-F and F-LDN-F, respectively, were highly localised to particular internal larval structures (Fig. 1K–N; Supplementary Fig. S1K–N). Miracidia exhibited weak immunoreactivity in the interepidermal ridge cytons and relatively intense reactivity in punctate patches distributed throughout the anterior half of the body (Fig. 1K and M). Using ImageJ software, z-stack projections and 3D visualisations of immunoreactive larval structures revealed that LDN-DF and DF-LDN-DF were present in the peripheral neurons of the miracidial neural mass and in the associated anterior, anterolateral and posterolateral sensory nerves (Fig. 3A). Micrographs of 2-day in vitro-cultivated primary sporocysts also show punctate clusters of strong anti-[DF]-LDN-DF immunoreactivity (Fig. 1L and N), but no defined structures were obvious in z-stack projections. However, imaging of 8-day sporocysts revealed strong

localisation in the syncytial body matrices, particularly at the peripheries of reticulum and/or germ cells (Supplementary Fig. S1K–N). This focal distribution was sustained through 21 days of cultivation in ccBge medium, although the expression of LDN-DF appears to wane at this later time point.

Confocal laser scanning microscopy and EFM data indicate that LDN-DF and DF-LDN-DF also are heterogeneously surfaceexpressed amongst miracidia (Fig. 2K and M; Supplementary Fig. S2E–L). Some miracidia were observed in EFM preparations to present these glycotopes on one or more individual epidermal plates, while localisation in others comprised only the interepidermal ridges and terebratorium. Interestingly, amongst individuals featuring immunopositive plates, LDN-DF was not observed on plate-associated cilia, but DF-LDN-DF invariably localised to both plate cells and cilia. More than half of the miracidia exhibited no surface immunoreactivity. Consistent with CLSM data that demonstrated LDN-DF and DF-LDN-DF in the sensory-associated structures of miracidia, some larvae were observed by EFM to express these glycotopes in the multiciliated sensory papillae, which occur in the interepidermal ridges between the second and third tiers of epidermal plates (Pan, 1980). However, most miracidia exhibited no reactivity in these or other surfaceexposed sensory structures. While CLSM data do not indicate the expression of LDN-DF and DF-LDN-DF on the tegument of early primary sporocysts (Fig. 1L and N), EFM revealed that LDN-DF alone commonly localised to the sporocyst tegument (Fig. 2L and N).

TriMan also was highly localised in the bodies of miracidia and primary sporocysts. In particular, CLSM micrographs and zstack projections demonstrated its presence in the miracidial lateral glands and terebratorium (Figs. 1O and 3B). Expression in the lateral glands was observed through 8 days of larval cultivation in CBSS+, but only traces remained following 21 days of cultivation in ccBge medium (Fig. 1P; Supplementary Fig. S1O and P). TriMan appears to also localise to a thin layer outside the superficial muscles of both larval stages (Fig. 1O and P; Supplementary Fig. S1O and P), although, as demonstrated by EFM (Fig. 2O and P), little or no surface staining strongly implies that this superficial reactivity is not attributable to the epidermal plates and tegument of miracidia and primary sporocysts, respectively. Interestingly, both CLSM and EFM detected TriMan on a subset of epidermal plate-associated cilia but not on the plate cells themselves.

3.2. Western blot analyses of larval whole-body and superficial extracts, epidermal plate proteins and LTPs

To determine whether glycotope-bearing proteins were released during larval transformation and to investigate the distribution of glycotopes amongst glycoproteins of miracidia and primary sporocysts, SDS–PAGE/Western blotting was applied to larval whole-body and surface-enriched protein extracts, isolated epidermal plate glycoproteins and LTPs. Immunoblots demonstrated the expression of all tested glycotopes except Lewis X on larval glycoproteins. Additionally, 1D and 2D blots revealed that glycotopes are presented on overlapping but quite distinct sets of larval proteins (Figs. 4 and 5).

Compared to control blots (Fig. 4A) non-fucosylated LDN was only weakly detected in whole-body extracts of both miracidia and primary sporocysts, particularly amongst proteins above ~37 kDa (Fig. 4B). Consistent with CLSM and EFM results, anti- LDN immunoreactivity was not observed amongst epidermal plate proteins or LTPs. Moreover, 2D analysis of miracidial and primary sporocyst surface-enriched protein extracts also produced weak blot patterns that comprised spots >37 kDa, but spots were spread over a broad pH range. Importantly, 2D blot patterns did not vary much between larval stages, suggesting only minor changes in LDN-bearing glycoprotein expression during larval transformation (data not shown).

Glycotopes F-LDN, F-LDN-F and LDN-F were well represented in whole-body and surface-enriched miracidial extracts, epidermal plate extracts and LTPs, with numerous glycoproteins ranging from >100 to ~10 kDa for F-LDN and F-LDN-F and >100 to ~25 kDa for LDN-F (Figs. 4C–E and 5A, B). One and 2D blot patterns indicate that many miracidial glycoproteins, especially those <37 kDa, were shed with the epidermal plates and as LTPs during larval transformation and thus were not detected in whole-body and surface-enriched extracts of 2-day primary sporocysts. Moreover, blots indicate that F-LDN and F-LDN-F are expressed on a shared set of glycoproteins, which is strikingly different from that featuring the LDN-F glycotope. Although some proteins seemingly present both F-LDN-[F] (referring to F-LDN and F-LDN-F collectively) and LDN-F, many proteins appear to express one or the other glycotope. Additionally, 2D blots of surface-enriched larval extracts suggest that while many F-LDN-[F] and LDN-F-bearing miracidial proteins are shed during larval transformation, relatively few glycotopebearing proteins are gained in primary sporocysts.

The LDN-DF and DF-LDN-DF glycotopes also were detected amongst whole-body and surface-enriched miracidial extracts, epidermal plate extracts and isolated LTPs, but only LDN-DF was observed in extracts of primary sporocysts (Figs. 4F, G and 5C). Their presence amongst epidermal plate proteins is consistent with CLSM and EFM data demonstrating their localisation in miracidial plates. Indeed, as indicated in 1D and 2D immunoblots of miracidial and sporocyst surface-enriched extracts, most superficial [DF]-LDN-DF-bearing miracidial proteins were shed during larval transformation and thus were generally absent in extracts of primary sporocysts. Specifically, miracidial extracts comprised multiple proteins >37 kDa featuring one or both glycotopes as well as robustly reactive acidic proteins ranging from ~17 to 27 kDa for LDN-DF and from ~22 to 32 kDa for DF-LDN-DF. All of these proteins were absent or only weakly detected in extracts of 2-day primary sporocysts. Immunoblots also demonstrated that [DF]-LDN-DF-bearing LTPs are largely plate-derived. Interestingly, despite their seemingly complete co-localisation in both miracidia and primary sporocysts, LDN-DF and DF-LDN-DF were presented on distinct sets of larval proteins, and their blot patterns to some degree resemble those for LDN-F and F-LDN-[F] glycotopes, respectively.

TriMan was observed in whole-body and surface-enriched extracts of both miracidia and primary sporocysts (Figs. 4H and 5D). Although CLSM and EFM data show that TriMan was expressed on epidermal plate-associated cilia, it was not detected in immunoblots of plate proteins and LTPs. Moreover, 2D blot patterns of miracidial and primary sporocyst proteins were quite similar, indicating that TriMan expression amongst superficially localised proteins was not greatly affected by epidermal plate shedding.

Both 1D and 2D immunoblots clearly show that glycotopes occur on distinct but overlapping sets of larval proteins such that at least some proteins potentially express multiple glycotopes. For example, mAbs against F-LDN-F, LDN-F and TriMan all reacted strongly against several proteins at ~48 kDa in 2D blots of superficially localised larval proteins (Fig. 5), implying the possibility that these proteins express all three glycotopes.

3.3. Western blot analysis of B. glabrata hemocyte and plasma glycoproteins

To further investigate the sharing of naturally occurring glycotopes between the early larval stages of *S. mansoni* and its snail intermediate host, *B. glabrata* hemocyte and plasma glycoproteins were PAGE-fractionated and immunoblotted using the anti-glycotope mAbs listed in Table 1. Comparable to the secondary antibody- only control (Fig. 6A) most glycotopes, including LDN, FLDN- F, LDN-F, LDN-DF, DF-LDN-DF and Lewis X, were not detected in hemocyte or plasma protein extracts. By contrast, TriMan was robustly detected in both snail hemolymph fractions (Fig. 6C), and F-LDN, which occurred on a distinct subset of glycoproteins, was detected primarily amongst plasma proteins. Anti-F-

LDN immunoreactivity against hemocyte proteins was relatively weak, being restricted to a single band at ~40 kDa (Fig. 6B).

4. Discussion

Carbohydrate-specific mAbs have emerged as an important tool for studies of schistosome glycobiology (Nibbeling et al., 1998; van Remoortere et al., 2000; Robijn et al., 2005; van Roon et al., 2005; Wuhrer et al., 2006; Lehr et al., 2008). In the present investigation, previously defined mAbs were used in immunofluorescence microscopy and Western blot analyses to examine the expression and localisation of schistosome-associated terminal CHO structures (glycotopes) in miracidia and primary sporocysts of *S. mansoni*.

The miracidium-to-primary sporocyst transformation is an important milestone in intramolluscan schistosome development. Following miracidial penetration, larvae shed their ciliated epidermal plates and form a syncytial tegument through the expansion of the miracidial interepidermal ridges (Samuelson and Caulfield, 1985; Chiang and Caulfield, 1988; Pan, 1996). During this process the developing larvae are vulnerable to the snail immune response and in resistant snails are encapsulated by circulating hemocytes and cytotoxically killed by the production of reactive oxygen and nitrogen intermediates (Owczarzak et al., 1980; Loker et al., 1982; Borges et al., 1998; Bayne et al., 2001; Hahn et al., 2001; Sasaki et al., 2005). Surface-expressed and excreted–secreted larval glycoconjugates have been implicated in modulating snail immunity and are thought ultimately to influence the outcome of infection (reviewed by El-Ansary, 2003), yet the contribution of their CHO constituents is still unclear. Moreover, while many studies have characterised the developmental expression of immunologically important glycotopes in mammalian host-associated developmental stages (van Remoortere et al., 2000, 2003; Wuhrer et al., 2002; Nyame et al., 2003; Robijn et al., 2005; van Roon et al., 2005), few studies until now have examined their expression in intramolluscan schistosome larvae.

Fucosylated CHO elements are prominently expressed on the surfaces of miracidia and primary sporocysts of *S. mansoni*. Consistent with previous findings (Hokke et al., 2007; Lehr et al., 2008), data presented in this study indicate that F-LDN, F-LDN-F, LDN-F, LDN-DF, DF-LDN-DF and TriMan, but not Lewis X, are expressed on the miracidial surface. However, in contrast to Lehr et al. (2008) who did not report surface localisation of non-fucosylated LDN in miracidia, we observed prominent anti-LDN immunoreactivity on the terebratorium and interepidermal ridges. Following larval transformation, only F-LDN, F-LDN-F, LDN-F and LDN-DF were retained on the sporocyst tegument, indicating a selective reduction in CHO structural diversity at the time of infection in the snail host. The coincidental loss of fucosylated LDN-reactive glycoproteins in sporocysts, especially lower mol. wt. proteins, and their appearance in epidermal plate extracts and LTPs strongly supports plates as a significant source of glycotopes released during larval transformation. Consistent with this result, Wu et al. (2009) showed that the majority of LTPs <25 kDa were highly periodate- sensitive (i.e., glycosylated), and many of these proteins were tentatively identified in subsequent proteomic analyses.

While some glycotopes were generally uniformly distributed on the miracidial surface, others, including LDN-F, LDN-DF and DFLDN- DF, exhibited substantial heterogeneity, with their localisation in the terebratorium, interepidermal ridges and epidermal plates varying from individual to individual in a single sample population. Interestingly, this sort of variation in glycotope expression also occurs amongst schistosomula (unpublished observation). A striking result of this study is the heterogeneity observed amongst miracidial epidermal plates such that antibodies reacted strongly or not at all to individual plates of a given miracidium. Although it is possible that these variations may be a technical artifact of

the fixation and staining process, it is important to note that these same variations were also observed in CLSM preparations and that only a subset of the investigated glycotopes exhibited these distribution patterns despite the larvae originating from a single fixed pool. Moreover, the occurrence of strongly immunopositive and wholly negative epidermal plates in individual miracidia suggests a biological phenomenon rather than a technical anomaly. With this in mind, heterogeneous expression in miracidia could also be attributable to differences in miracidial age and developmental status (i.e., older individuals naturally accumulate or shed surface-localised LDN-F, LDN-DF and DF-LDN-DF), which are a consequence of the egg isolation technique used in this investigation. Eggs were obtained from infected mouse livers rather than fresh feces, and the gradual accumulation of eggs in the liver over time results in variation of age and development amongst miracidia obtained by this method. Alternatively, heterogeneous glycotope expression may be a natural phenomenon by which some but not all miracidia (or epidermal plates) express LDN-F, LDN-DF and DF-LDN-DF. Importantly, the presence/absence or relative abundance of these glycotopes on the miracidial surface may influence the ability of individuals to establish an infection in the snail intermediate host. How such heterogeneity in glycotope expression might arise is unclear, but it undoubtedly reflects qualitative and/or quantitative differences in the fucosyltransferase activities required for oligosaccharide synthesis. Additionally, the expression of the protein or lipid carriers for particular glycotopes and/or the occurrence of GDP-Fuc donor and glycan acceptor substrates may be differentially distributed amongst miracidia or their epidermal plates.

Glycotopes also localised in larval structures within the bodies of miracidia and primary sporocysts, with some glycotopes exhibiting broad internal distributions (e.g., LDN) and others occurring more focally in specific organs (e.g., LDN-DF, DF-LDN-DF, TriMan). For example, LDN-DF and DF-LDN-DF glycotopes, which bear a unique Fucα1-2Fuc linkage, were presented on the neural mass and associated sensory nerves of miracidia and in the body matrices of primary sporocysts. The miracidial sensory nerves are thought to act as chemoreceptors, mechanoreceptors, photoreceptors and/or depth sensors and presumably function in host-seeking and penetration (Pan, 1980; Eklu-Natey et al., 1985), but the specific role of Fucα2Fucα3-substituted LDN glycotopes in these processes, if any, is unknown. Moreover, as was evident by the re-organisation of LDN-DF and DF-LDN-DF in early primary sporocysts, these miracidial sensory structures are dismantled during larval transformation and sporocyst development (Schutte, 1974; Koie and Frandsen, 1976; Pan, 1996).

TriMan also featured a focal distribution in miracidia. Specifically, TriMan was prominently expressed in the miracidial lateral glands, which secrete lytic enzymes that are thought to assist egg translocation between blood vessels and the gut lumen in definitive hosts and contribute to miracidial penetration of the snail intermediate host (Pino-Heiss et al., 1985; Sturrock, 2001). As evident by the retention of internally localised TriMan in 8- day primary sporocysts, the lateral glands persist throughout early sporocyst development (Schutte, 1974). Moreover, Pan (1980) noted that these glandular cells continue to release their secretory products into surrounding snail tissues for several days following the initiation of transformation. Our analysis, however, failed to detect TriMan in immunoblots of parasite culture supernatants containing LTPs, probably reflecting differences between in vivo and in vitro larval behaviour or the differing affinities of mAb 100-4G11-A in microscopy versus immunoblot analyses.

In addition to determining glycotope localisation, glycotope expression amongst larval glycoproteins, particularly those that are surface-associated and/or released during larval transformation, also was investigated. One and 2D immunoblots generally complemented CLSM and EFM data, demonstrating the expression of all but the Lewis X glycotope in

protein extracts of both miracidia and primary sporocysts. Blots also confirmed that variously fucosylated LDN glycotopes, but not non-fucosylated LDN, occur on miracidial epidermal plate proteins and LTPs that presumably are released from plates undergoing lysis following transformation (Wu et al., 2009). In contrast, although TriMan was observed by EFM on a subset of plate-associated cilia, it was not detected amongst plate proteins or LTPs. TriMan occurs only as an N-linked glycan (van Remoortere et al., 2003); thus its presence with plateassociated proteins was expected. However, due to its limited ciliary localisation, TriMan-bearing proteins likely represent a relatively minor portion of plate-isolated proteins, possibly explaining their absence in immunoblots.

In terms of larval transformation, although EFM data indicate that glycotope surface localisation did not change greatly from miracidia to primary sporocysts, 2D immunoblots of surface-enriched larval extracts generally demonstrated the loss of many glycotope-bearing proteins without a reciprocal gain of new protein expression in primary sporocysts. One-dimensional blots suggest that most of the proteins lost during larval transformation are plate-associated and are ultimately released as LTPs. Many glycotope- bearing proteins appear to be expressed by both larvae.

Consistent with previous investigations of glycotope expression in mammalian host-associated developmental stages (Nyame et al., 2003; Robijn et al., 2005), different structures frequently were detected in 1D and 2D immunoblots on overlapping but distinct sets of glycoproteins. In fact, blot-to-blot comparisons often revealed relatively few immunopositive proteins that were shared features between two or more blots. Interestingly, in some cases blot profile differences were not accompanied by differences in EFM and CLSM localisation. For example, both LDN-DF and DF-LDN-DF co-localised in the neural mass, sensory nerves and epidermal plates of miracidia, but immunoblots revealed their expression on distinct protein sets. Moreover, LDN-DF and DF-LDN-DF blot profiles resemble those of LDN-F and F-LDN-F, respectively, which exhibit a localisation pattern that is distinct (or different) from that of Fucα2Fucα3- substituted LDN. Importantly, these observations imply that localisation alone cannot explain such protein-specific glycosylation patterns. Nyame et al. (2003) in a similar set of localisation and blot profiling experiments demonstrated that LDN, LDN-F and Lewis X co-localise on the surfaces of cercariae, schistosomula and adults of *S. mansoni*, but immunoblots revealed distinct glycosylation patterns for each glycotope in these developmental stages. As noted in this previous work, the underlying mechanism of selective glycosylation is not well understood. Glycosylated proteins are generally passaged along a common secretory pathway and are thought to have equal opportunity for such post-translational modifications (Colley, 1997; Opat et al., 2001). A possible mechanism following this premise is that protein backbones, which vary in size, conformation and charge, are differentially utilised as substrates by endoplasmic reticulum (ER)- and Golgi-resident glycosyltransferases. In this scenario protein backbones and glycosyltransferases are not spatially segregated, but protein–transferase interactions are restricted. Alternatively, the opposite may be true, with protein backbones and glycosyltransferases selectively segregating into ER and Golgi compartments (i.e., the admission of both glycosyltransferases and protein substrates to particular compartments is restricted) while protein–transferase interactions occur freely within compartments. Fully explaining the observed localisation and blot patterns likely involves the co-occurrence of multiple specific fucosyltransferases either functionally or spatially “compartmentalised” with their protein substrates.

The resemblance of LDN-DF and DF-LDN-DF blot patterns to those of LDN-F and F-LDN-F, respectively, may not be surprising given these structures presumably result from the coordinated efforts of multiple fucosyltransferases, each capable of producing a particular glycosidic linkage. Indeed, a keyword search for “fucosyltransferase” in the schistosome

genomic database (www.SchistoDB.org) yielded multiple predicted fucosyltransferase genes. Given the multiplicity of the fucosylation machinery and the potential for functional or spatial compartmentalisation, one could hypothesise a mechanism to explain some or all of these observations. However, without additional information any such proposal would be highly speculative. Regardless, the present investigation clearly demonstrates the underlying complexity of schistosome glycosylation.

As previously mentioned, host lectins are thought to act as pathogen recognition receptors (Glinski and Jarosz, 1997; Janeway and Medzhitov, 2002; Vasta et al., 2007) and, therefore, one of the objectives of the present study was to profile the glycan repertoire presented to the snail host by early infecting larval schistosomes to begin assessing the role of specific glycotopes in promoting or suppressing snail immune activity. Previous studies suggest that shared glycan elements, particularly those featuring a terminal Fucα1-3GalNAc linkage, i.e., F-LDN and F-LDN-F, possibly mediate CHO-based molecular mimicry between larval schistosomes and *B. glabrata* (Lehr et al., 2007, 2008), which is thought to be a parasite strategy for immune evasion (Yoshino and Bayne, 1983; Bayne et al., 1987; Damian, 1989). Although the present investigation did not detect F-LDN-F or LDN-F on snail hemocyte and plasma glycoproteins, it did confirm the expression of F-LDN in both *B. glabrata* and intramolluscan schistosome larvae. While the lack of F-LDN-F and LDN-F in our immunoblots may be explained simply by insufficient protein load, an alternative explanation could be that differences in glycotope expression are associated with our use of hemolymph from a different snail strain. In fact, previous investigations by Lehr et al. (2007, 2008) employed a susceptible strain of *B. glabrata*, whereas the BS90 strain of resistant snails was used in the present study. Interestingly, both F-LDN-F and LDN-F have a Fucα1- 3GlcNAc structural motif not found in F-LDN (see Table 1). Moreover, this linkage in both glycotopes is likely produced by a single fucosyltransferase, allowing the possibility that, if indeed snail strains differ in terms of glycotope presentation, strain-specific differences may occur at the level of fucosyltransferase gene expression. Therefore an investigation to directly assess strain-specific glycotope expression in *B. glabrata* is warranted.

In addition to α3-fucosylated LDN, TriMan also was found in both *B. glabrata* and schistosome larvae. Its presence amongst snail plasma glycoproteins is consistent with mass spectrometry data presented by Lehr et al. (2007). Although CLSM and EFM revealed only weak surface anti-TriMan immunoreactivity in either larval stage, this glycotope strongly localised between the miracidial epidermal plates/sporocyst tegument and the subtending circular muscle layer, a region in both larvae that corresponds to an acellular basal lamina (Pan, 1980). While some studies (Meuleman et al., 1978; Samuelson and Caulfield, 1985) have demonstrated synchronisation of miracidial plate shedding and expansion of the interepidermal ridges, Pan (1980) observed in vivo that the plates may be torn from the miracidium by reactive snail hemocytes before the primary sporocyst tegument has fully formed. The basal lamina may therefore be exposed to the host milieu during natural infections, providing an opportunity for TriMan to play a role in CHO-based molecular mimicry at this temporary snail–schistosome interface.

Carbohydrate-based molecular mimicry implies evolutionary convergence in compatible parasite–host systems. However, strain-specific susceptibility and resistance in schistosome–snail interactions has been well documented for *Biomphalaria* (e.g., Richards and Merritt, 1972; Frandsen, 1979; Incani, 1993). Previous studies have reported strain-specific differences in the hemocyte anti-CHO immune response and variation of lectin reactivity to the surfaces of hemocytes from susceptible and resistant snails (indicating differences in CHO content) (Boswell and Bayne, 1985; Martins-Souza et al., 2006), suggesting that CHOs potentially play a role in compatibility polymorphism between *S. mansoni* and its

snail intermediate host. Theron and Coustau (2005) hypothesised that compatibility is tested at the level of individuals, with the success or failure of an infection being determined not by the susceptibility/resistance of the snail itself, but on the "matched" or "mismatched" status of the phenotypes of the invading larva and its host snail. In other words, the resistance or susceptibility of a given snail (or snail strain) is not absolute. In the context of glycotope expression, this might mean that susceptibility/resistance of a snail depends on whether or not the invading miracidium expresses proteins and lipids with matching, i.e., compatible, CHO structures on its surface. In essence, schistosome larvae must don an appropriate camouflage to avoid detection in the snail milieu. Given the complexity of these parasite–host interactions, an investigation that examines snail-specific glycotope expression should also compare compatible and incompatible strains of *S. mansoni*.

Supplementary Material

Refer to Web version on PubMed Central for supplementary material.

Acknowledgments

The authors thank the W.M. Keck Laboratory for Biological Imaging, School of Medicine and Public Health, University of Wisconsin – Madison (USA), especially Lance Rodenkirch for his technical advice. This work was supported by NIH Grants AI015503 and AI061436 to T.P.Y. and NIH schistosomiasis supply contract AI30026 (F. Lewis, Biomedical Research Institute, Rockville, MD, USA). N.A.P. is currently a NIH predoctoral fellow supported by NIH T32 AI007414.

References

Bahia D, Avelar LGA, Vigarosi F, Cioli D, Oliveira GC, Mortara RA. The distribution of motor proteins in the muscles and flame cells of the *Schistosoma mansoni* miracidium and primary sporocyst. Parasitology. 2006; 133:321– 329. [PubMed: 16740180]

Bayne CJ, Boswell CA, Yui MA. Widespread antigenic cross-reactivity between plasma proteins of a gastropod, and its trematode parasite. Dev Comp Immunol. 1987; 11:321–329. [PubMed: 2442042]

Bayne CJ, Hahn UK, Bender RC. Mechanisms of molluscan host resistance and of parasite strategies for survival. Parasitology. 2001; 123:S159–S167. [PubMed: 11769280]

Berkelman, T.; Stenstedt, T. 2-D Electrophoresis using Immobilized pH Gradients: Principles and Methods. Amersham Pharmacia Biotech; Uppsala: 1998.

Borges CM, de Souza CP, Andrade ZA. Histopathologic features associated with susceptibility and resistance of *Biomphalaria* snails to infection with *Schistosoma mansoni*. Mem Inst Oswaldo Cruz. 1998; 93 (S1):117–121. [PubMed: 9921332]

Boswell CA, Bayne CJ. *Schistosoma mansoni*: lectin-dependent cytotoxicity of hemocytes from susceptible host snails, *Biomphalaria glabrata*. Exp Parasitol. 1985; 60:133–138. [PubMed: 4040473]

Castillo MG, Wu XJ, Dinguirard N, Nyame AK, Cummings RD, Yoshino TP. Surface membrane proteins of *Biomphalaria glabrata* embryonic cells bind fucosyl determinants on the tegumental surface of *Schistosoma mansoni* primary sporocysts. J Parasitol. 2007; 93:832–840. [PubMed: 17918362]

Chiang CP, Caulfield JP. *Schistosoma mansoni*: ultrastructural demonstration of a glycocalyx that cross-reacts with antibodies raised against the cercarial glycocalyx. Exp Parasitol. 1988; 67:63–72. [PubMed: 2458959]

Chernin E. Observations on hearts explanted in vitro from the snail *Australorbis glabratus*. J Parasitol. 1963; 49:353–364. [PubMed: 14020610]

Chitsulo L, Engels D, Montresor A, Savioli L. The global status of schistosomiasis and its control. Acta Trop. 2000; 77:41–51. [PubMed: 10996119]

Colley KJ. Golgi localization of glycosyltransferases: more questions than answers. Glycobiology. 1997; 7:1–13. [PubMed: 9061359]

Damian RT. Molecular mimicry: parasite evasion and host defense. Curr Top Microbiol Immunol. 1989; 145:101–115. [PubMed: 2553336]

Dunn TS, Yoshino TP. *Schistosoma mansoni*: origin and expression of a tegumental surface antigen on the miracidium and primary sporocyst. Exp Parasitol. 1988; 67:167–181. [PubMed: 2461313]

Eberl M, Langermans JAM, Vervenne RA, Nyame AK, Cummings RD, Thomas AW, Coulson PS, Wilson RA. Antibodies to glycans dominate the host response to schistosome larvae and eggs: is their role protective or subversive? J Infect Dis. 2001; 183:1238–1247. [PubMed: 11262206]

Eklu-Natey DT, Wuest J, Swiderski Z, Striebel HP, Huggel H. Comparative scanning electron microscope (SEM) study of four human schistosome species. Int J Parasitol. 1985; 15:33–42. [PubMed: 3980140]

El-Ansary A. Biochemical and immunological adaptation in schistosome parasitism. Comp Biochem Physiol B: Biochem Mol Biol. 2003; 136:227–243. [PubMed: 14529749]

Frandsen F. Studies of the relationship between *Schistosoma mansoni* and their intermediate hosts: III. The genus *Biomphalaria* and *Schistosoma mansoni* from Egypt, Kenya, Sudan, Uganda, West Indies (St Lucia) and Zaire (two different stains: Katanga and Kinshasa). J Helminthol. 1979; 53:321– 348. [PubMed: 541498]

Glinski Z, Jarosz J. Molluscan immune defenses. Arch Immunol Ther Exp (Warsz). 1997; 45:149–155. [PubMed: 9597080]

Hahn UK, Bender RC, Bayne C. Production of reactive oxygen species by haemocytes of *Biomphalaria glabrata*: carbohydrate-specific stimulation. Dev Comp Immunol. 2000; 24:531–541. [PubMed: 10831788]

Hahn UK, Bender RC, Bayne CJ. Killing of *Schistosoma mansoni* sporocysts by hemocytes from resistant *Biomphalaria glabrata*: role of reactive oxygen species. J Parasitol. 2001; 87:292–299. [PubMed: 11318558]

Hokke CH, Deelder AM, Hoffmann KF, Wuhrer M. Glycomics-driven discoveries in schistosome research. Exp Parasitol. 2007; 117:275–283. [PubMed: 17659278]

Incani RN. Compatibility of one Brazilian and two Venezuelan strains of *Schistosoma mansoni* with various strains of *Biomphalaria glabrata*. Parasitol Res. 1993; 79:508–511. [PubMed: 8415568]

Jacobs W, van Dam G, Bogers J, Deelder AM, van Marck E. Schistosomal granuloma modulation: I. *Schistosoma mansoni* worm antigens CAA and CCA prime egg-antigen-induced hepatic granuloma formation. Parasitol Res. 1999a; 85:7– 13. [PubMed: 9950221]

Jacobs W, Deelder AM, van Marck E. Schistosomal granuloma modulation: II. Specific immunogenic carbohydrates can modulate schistosome-egg-antigen-induced hepatic granuloma formation. Parasitol Res. 1999b; 85:14–18. [PubMed: 9950222]

Janeway CA, Medzhitov R. Innate immune recognition. Annu Rev Immunol. 2002; 20:197–216. [PubMed: 11861602]

Koie M, Frandsen F. Stereoscan observations of the miracidium and early sporocyst of *Schistosoma mansoni*. Z Parasitenkd. 1976; 50:335–344. [PubMed: 997727]

Lehr T, Geyer H, Maass K, Doenhoff MJ, Geyer R. Structural characterization of N-glycans from the freshwater snail *Biomphalaria glabrata* cross-reacting with *Schistosoma mansoni* glycoconjugates. Glycobiology. 2007; 17:82– 103. [PubMed: 16971380]

Lehr T, Beuerlein K, Doenhoff MJ, Grevelding CG, Geyer R. Localization of carbohydrate determinants common to *Biomphalaria glabrata* as well as to sporocysts and miracidia of *Schistosoma mansoni*. Parasitology. 2008; 135:931–942. [PubMed: 18507884]

Lejoly-Boisseau H, Appriou M, Seigneur M, Pruvost A, Tribouley-Duret J, Tribouley J. *Schistosoma mansoni*: in vitro adhesion of parasite eggs to the vascular endothelium. Subsequent inhibition by a monoclonal antibody directed to a carbohydrate epitope. Exp Parasitol. 1999; 91:20–29. [PubMed: 9920039]

Loker ES, Bayne CJ, Buckley PM, Kruse KT. Ultrastructure of encapsulation of *Schistosoma mansoni* mother sporocysts by hemocytes of juveniles of the 10-R2 strain of *Biomphalaria glabrata*. J Parasitol. 1982; 68:84–94. [PubMed: 7077450]

Martins-Souza RL, Pereira CA, Martins Filho OA, Coelho PH, Correa A Jr, Negrao-Correa D. Differential lectin labeling of circulating hemocytes from *Biomphalaria glabrata* and *Biomphalaria*

tenegophila resistant and susceptible to *Schistosoma mansoni* infection. Mem Inst Oswaldo Cruz. 2006; 101 (1):185–192. [PubMed: 17308768]

Meuleman EA, Lyaruu DM, Khan MA, Holzmann PJ, Sminia T. Ultrastructural changes in the body wall of *Schistosoma mansoni* during the transformation of the miracidium into the mother sporocyst in the snail host *Biomphalaria pfeifferi*. Z Parasitenkd. 1978; 56:227–242. [PubMed: 695828]

Nibbeling HAM, Kahama AI, van Zeyl RJM, Deelder AM. Use of monoclonal antibodies prepared against *Schistosoma mansoni* hatching fluid antigens for demonstration of *Schistosoma haematobium* circulating egg antigens in urine. Am J Trop Med Hyg. 1998; 58:543–550. [PubMed: 9598438]

Nolan LE, Carriker JP. Observations on the biology of the snail *Lymnaea stagnalis appressa* during twenty years of laboratory culture. Am Midl Nat. 1946; 36:467–493.

Nyame AK, Yoshino TP, Cummings RD. Differential expression of LacdiNAc, fucosylated LacdiNAc, and Lewis x glycan antigens in intramolluscan stages of *Schistosoma mansoni*. J Parasitol. 2002; 88:890–897. [PubMed: 12435126]

Nyame AK, Lewis FA, Doughty BL, Correa-Oliveira R, Cummings RD. Immunity to schistosomiasis: glycans are potential antigenic targets for immune intervention. Exp Parasitol. 2003; 104:1–13. [PubMed: 12932753]

Opat AS, van Vliet C, Gleeson PA. Trafficking and localization of resident Golgi glycosylation enzymes. Biochimie. 2001; 83:763–773. [PubMed: 11530209]

Owczarzak A, Stibbs HH, Bayne CJ. The destruction of *Schistosoma mansoni* mother sporocysts in vitro by amoebae isolated from *Biomphalaria glabrata*: an ultrastructural study. J Invertebr Pathol. 1980; 35:26–33. [PubMed: 7365267]

Pan SC. The fine structure of the miracidium of *Schistosoma mansoni*. J Invertebr Pathol. 1980; 36:307–372. [PubMed: 7452064]

Pan SC. *Schistosoma mansoni*: the ultrastructure of larval morphogenesis in *Biomphalaria glabrata* and of associated host–parasite interactions. Jpn J Med Sci Biol. 1996; 49:129–149. [PubMed: 9086392]

Pino-Heiss S, Brown M, McKerrow JH. *Schistosoma mansoni*: degradation of host extracellular matrix by eggs and miracidia. Exp Parasitol. 1985; 59:217–221. [PubMed: 3882446]

Plows LD, Cook RT, Davies AJ, Walker AJ. Activation of extracellularsignal regulated kinase is required for phagocytosis by *Lymnaea stagnalis* haemocytes. Biochim Biophys Acta. 2004; 28:25–33. [PubMed: 15158361]

Plows LD, Cook RT, Davies AJ, Walker AJ. Carbohydrates that mimic schistosome surface coat components affect ERK and PKC signaling in *Lymnaea stagnalis* haemocytes. Int J Parasitol. 2005; 35:293–302. [PubMed: 15722081]

Richards CJ, Merritt JW Jr. Genetic factors in the susceptibility of juvenile *Biomphalaria glabrata* to *Schistosoma mansoni* infection. Am J Trop Med Hyg. 1972; 21:425–434. [PubMed: 5050093]

Robijn ML, Wuhrer M, Kornelis D, Deelder AM, Geyer R, Hokke CH. Mapping fucosylated epitopes on glycoproteins and glycolipids of *Schistosoma mansoni* cercariae, adult worms, and eggs. Parasitology. 2005; 130:67–77. [PubMed: 15700758]

Robijn MLM, Koeleman CAM, Wuhrer M, Royle L, Geyer R, Dwek RA, Rudd PM, Deelder AM, Hokke CH. Targeted identification of a unique glycan epitope of *Schistosoma mansoni* egg antigens using a diagnostic antibody. Mol Biochem Parasitol. 2007; 151:148–161. [PubMed: 17188765]

Ross AGP, Bartley PB, Sleigh AC, Olds GR, Li Y, Williams GM, McManus DP. Schistosomiasis. N Engl J Med. 2002; 346:1212–1220. [PubMed: 11961151]

Sambrook, J.; Fritsch, EF.; Maniati, T. SDS–polyacrylamide gel electrophoresis of proteins. In: Ford, N.; Nolan, C.; Ferguson, M., editors. Molecular Cloning: A Laboratory Manual. Cold Spring Harbor Laboratory Press; 1989. p. 18.47-18.54.

Samuelson JC, Caulfield JP. Role of pleated septate junctions in the epithelium of miracidia of *Schistosoma mansoni* during transformation to sporocysts in vitro. Tissue Cell. 1985; 17:667–682. [PubMed: 4060143]

Sasaki Y, Kirinoki M, Chigusa Y. Comparative studies of the defense mechanism against *Schistosoma japonicum* of schistosome-susceptible and - resistant *Oncomelania nosophora*. Parasitol Int. 2005; 54:157–165. [PubMed: 15897002]

Schutte CHJ. Studies on the South African strain of *Schistosoma mansoni*: Part 2. The intra-molluscan larval stages. S Afr J Sci. 1974; 70:327–346.

Sminia T, Barendsen LA. A comparative morphological and enzyme histochemical study on blood cells of the freshwater snails *Lymnaea stagnalis*, *Biomphalaria glabrata* and *Bulinus truncatus*. J Morphol. 1980; 165:31–39.

Steinmann P, Keiser J, Bos R, Tanner M, Utzinger J. Schistosomiasis and water resources development: systemic review, meta analysis, and estimates of people at risk. Lancet Infect Dis. 2006; 6:411–425. [PubMed: 16790382]

Sturrock, RF. The schistosomes and their intermediate hosts. In: Mahmoud, AAF., editor. Schistosomiasis. Imperial College Press; London: 2001. p. 7-84.

Theron A, Coustau C. Are *Biomphalaria* snails resistant to *Schistosoma mansoni*? J Helminthol. 2005; 79:187–191. [PubMed: 16153311]

Van de Vijver KK, Hokke CH, van Remoortere A, Jacobs W, Deelder AM, van Marck EA. Glycans of *Schistosoma mansoni* and keyhole limpet haemocyanin induce hepatic granulomas in vivo. Int J Parasitol. 2004; 34:951–961. [PubMed: 15217734]

Van de Vijver KK, Deelder AM, Jacobs W, van Mark EA, Hokke CH. LacdiNAc and LacNAc-containing glycans induce granulomas in an *in vivo* model for schistosome egg-induced hepatic granuloma formation. Glycobiology. 2006; 16:237–243. [PubMed: 16282603]

van Remoortere A, Hokke CH, van Dam GJ, van Die I, Deelder AM, van den Eijnden DH. Various stages of Schistosoma express LewisX, LacdiNAc, GalNAcb1-4(Fuca1-3)GlcNAc, and GalNAcb1-4(Fuca1-2Fuca1-3)GlcNAc carbohydrate epitopes: detection with monoclonal antibodies that are characterized enzymatically synthesized neoglycoproteins. Glycobiology. 2000; 10:601–609. [PubMed: 10814702]

van Remoortere A, Bank CMC, Nyame AK, Cummings RD, Deelder AM, van Die I. *Schistosoma mansoni*-infected mice produce antibodies that crossreact with plant, insect, and mammalian glycoproteins and recognize the truncated biantennary N-glycan Man3GlcNAc2. Glycobiology. 2003; 13:217–225. [PubMed: 12626421]

van Roon AMM, Aguilera B, Cuenca F, van Remoortere A, van der Marel GA, Deelder AM, Overkleeft HS, Hokke CH. Synthesis and antibodybinding of a series of parasite fuco-oligosaccharides. Bioorg Med Chem. 2005; 13:3553–3564. [PubMed: 15848768]

Vasta GR, Ahmed H, Tasumi S, Odom EW, Saito K. Biological roles of lectins in innate immunity: molecular and structural basis for diversity in self/non-self recognition. Adv Exp Med Biol. 2007; 598:389–406. [PubMed: 17892226]

Vermeire JJ, Boyle JP, Yoshino TP. Differential gene expression and the effects of *Biomphalaria glabrata* embryonic (Bge) cell factors during larval *Schistosoma mansoni* development. Mol Biochem Parasitol. 2004; 135:153–157. [PubMed: 15287597]

Wu X, Sabat G, Brown JF, Zhang M, Taft A, Peterson N, Harms A, Yoshino TP. Proteomic analysis of *Schistosoma mansoni* proteins released during in vitro miracidium-to-sporocyst transformation. Mol Biochem Parasitol. 2009; 164:32–44. [PubMed: 19095013]

Wuhrer M, Kantelhardt SR, Dennis RD, Doenhoff MJ, Lochnit G, Geyer R. Characterization of glycosphingolipids from *Schistosoma mansoni* eggs carrying Fuc(a1-3)GalNAc-, GalNAc(b1-4)[Fuc(a1-3)]GalNAc- and Gal(b1- 4)[Fuc(a1-3)]GalNAc- (Lewis X) terminal structures. Eur J Biochem. 2002; 269:481–493. [PubMed: 11856306]

Wuhrer M, Koeleman CA, Fitzpatrick JM, Hoffmann KF, Deelder AM, Hokke CH. Gender-specific expression of complex-type N-glycans in schistosomes. Glycobiology. 2006; 16:991–1006. [PubMed: 16825488]

Yoshino TP, Bayne CJ. Mimicry of snail host antigens by miracidia and primary sporocysts of *Schistosoma mansoni*. Parasite Immunol. 1983; 5:317– 328. [PubMed: 6191268]

Yoshino TP, Laursen JR. Production of *Schistosoma mansoni* daughter sporocysts from mother sporocysts maintained in synxenic culture with *Biomphalaria glabrata* embryonic (Bge) cells. J Parasitol. 1995; 81:714–722. [PubMed: 7472861]

Yoshino TP, Dinguirard N, Kunert J, Hokke CH. Molecular and functional characterization of a tandem-repeat galectin from the freshwater snail *Biomphalaria glabrata*, intermediate host of the human blood fluke *Schistosoma mansoni*. Gene. 2008; 411:46–58. [PubMed: 18280060]

Appendix A. Supplementary data

Supplementary data associated with this article can be found, in the online version, at doi: 10.1016/j.ijpara.2009.06.002.

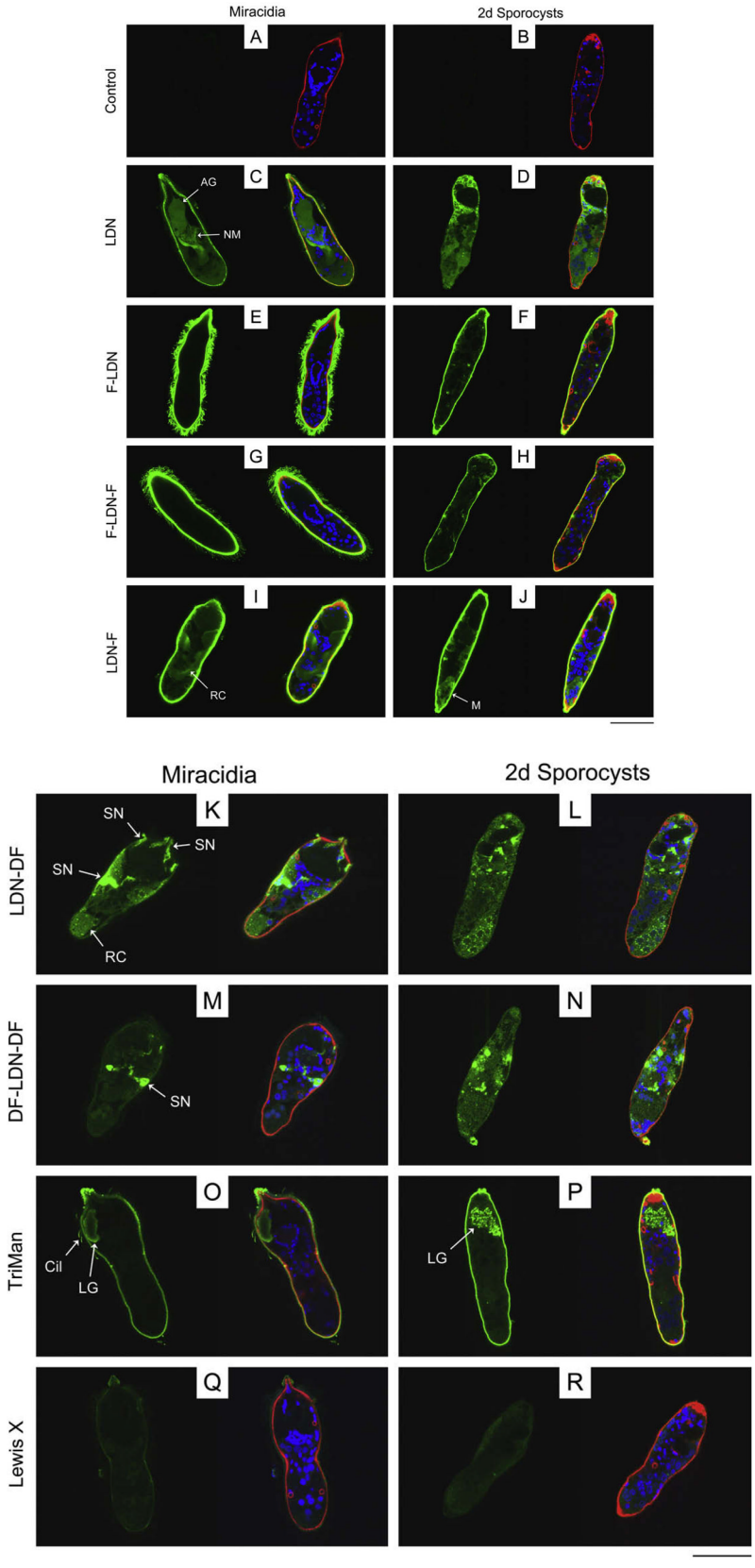

Fig. 1.

Localisation of glycotope expression in miracidia and primary sporocysts of *Schistosoma mansoni*. Confocal laser scanning microscopy was used to assess the localisation of schistosome-associated carbohydrate terminal structures in miracidia and 2-day (2d) in vitro-cultivated primary sporocysts. Fixed and permeabilised larvae were immunostained with monoclonal antibodies recognising GalNAcβ1-4GlcNAc (LDN; (C and D)), Fucα1-3GalNAcβ1-4GlcNAc (F-LDN; (E and F)), Fucα1-3GalNAcβ1- 4(Fucα1-3)GlcNAc (F-LDN-F; (G and H)), GalNAcβ1-4(Fucα1-3)GlcNAc (LDN-F; (I and J)), GalNAcβ1-4(Fucα1-2Fucα1-3)GlcNAc (LDN-DF; (K and L)), Fucα1-2Fucα1-3GalNAcβ1-4(Fucα1-2Fucα1-3)GlcNAc (DF-LDN-DF; (M and N)), Manα1-3(Manα1-6)Manβ1-4GlcNAcβ1-4GlcNAcβ1-Asn (TriMan; (O and P)) and Galβ1-4(Fucα1-3)GlcNAc (Lewis X; (Q and R)). Control larvae were exposed to secondary antibody without previous primary antibody treatment (A and B). Panels include paired micrographs depicting glycotope expression (green) alone and merged with counterstained actin (e.g., muscles, flame cells; red) and DNA (e.g., nuclei; blue). Approximate scale is represented in the lower right corner (bar = 50 μm). AG, apical gland; Cil, cilia; LG, lateral gland; M, sporocyst matrix; NM, neural mass; RC, interepidermal ridge cyton; SN, sensory nerve.

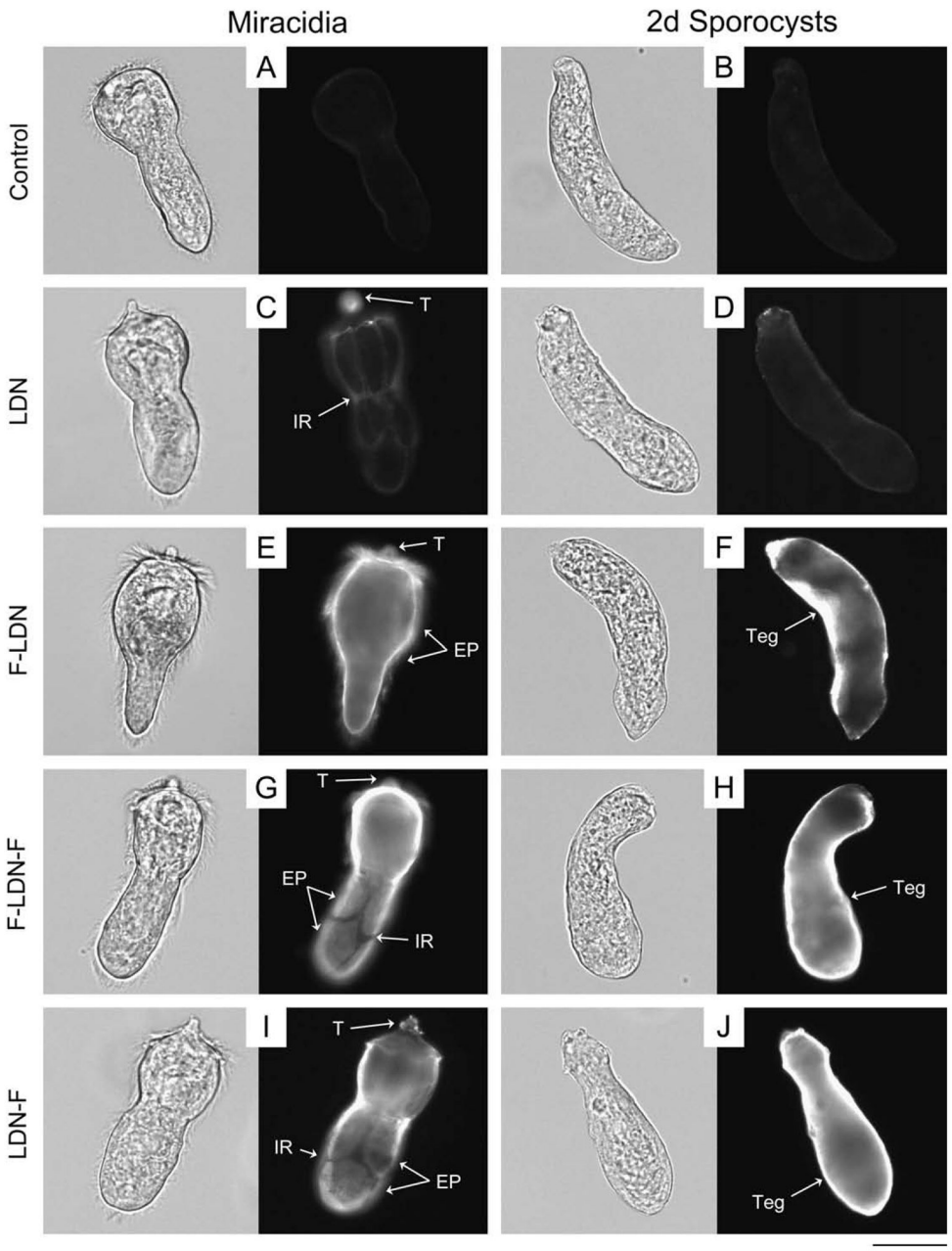

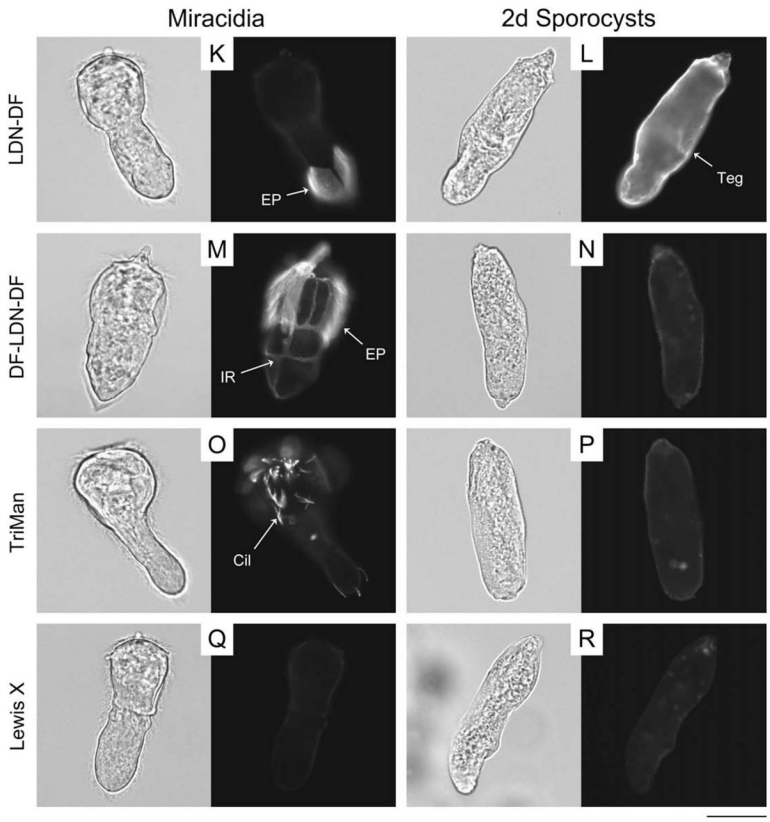

Fig. 2.

Glycotope expression on the exposed surfaces of miracidia and primary sporocysts of *Schistosoma mansoni*. The exposed surfaces of miracidia and 2-day (2d) in vitrocultivated primary sporocysts were examined for the expression of schistosome-associated carbohydrate terminal structures using epifluorescence microscopy. Fixed but non-permeabilised larvae were treated with monoclonal antibodies that recognise GalNAcβ1-4GlcNAc (LDN; (C and D)), Fucα1-3GalNAcβ1-4GlcNAc (F-LDN; (E and F)), Fucα1-3GalNAcβ1-4(Fucα1-3)GlcNAc (F-LDN-F; (G and H)), GalNAcβ1-4(Fucα1-3)GlcNAc (LDN-F; (I and J)), GalNAcβ1-4(Fucα1-2Fucα1-3)GlcNAc (LDN-DF; (K and L)), Fucα1-2Fucα1-3GalNAcβ1-4(Fucα1-2Fucα1-3)GlcNAc (DF-LDN-DF; (M and N)), Manα1-3(Manα1-6)Manβ1-4GlcNAcβ1-4GlcNAcβ1-Asn (TriMan; (O and P)) and Galβ1- 4(Fucα1-3)GlcNAc (Lewis X; (Q and R)). Control larvae were exposed to secondary antibody without previous primary antibody treatment (A and B). Micrographs depict glycotope expression patterns that were generally observed for each treatment, however larvae exhibited considerable heterogeneity regarding the expression of several glycotopes, particularly LDN-F, LDN-DF and DF-LDN-DF (see Supplementary Fig. S2). Panels include paired brightfield and fluorescence micrographs of individual larvae. Approximate scale is represented in the lower right corner (bar = 50 μm). Cil, cilia; EP, epidermal plate; IR, interepidermal ridge; T, terebratorium; Teg, tegument.

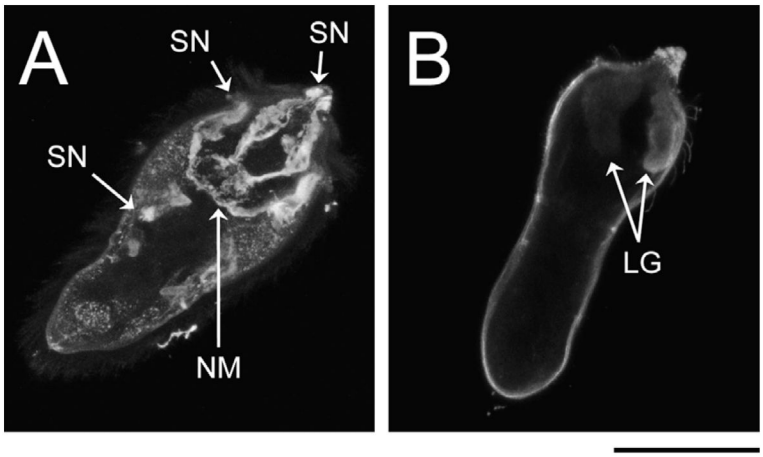

Fig. 3.

Confocal laser scanning microscopy (CLSM) z-stack projections of immunoreactive glycotope-bearing structures in miracidia of *Schistosoma mansoni*. To better visualise immunoreactive structures, individual miracidia were optically sectioned, creating a series of CLSM micrographs (z-stack) depicting sequential focal planes (1 to *n*). (A) S.D. z-stack projection (images 45–82, $n = 127$) of anti-LDN-DF (GalNAcβ1-4(Fucα1-2Fucα1-3)GlcNAc) immunoreactivity in miracidia; (B) S.D. projection (images 1–70, $n = 118$) of anti-TriMan (Manα1-3(Manα1-6)Manβ1-4GlcNAcβ1-4GlcNAcβ1-Asn) immunoreactivity in miracidia. Approximate scale is represented in the lower right corner (bar = 50 μm). LG, lateral gland; NM, neural mass; SN, sensory nerve.

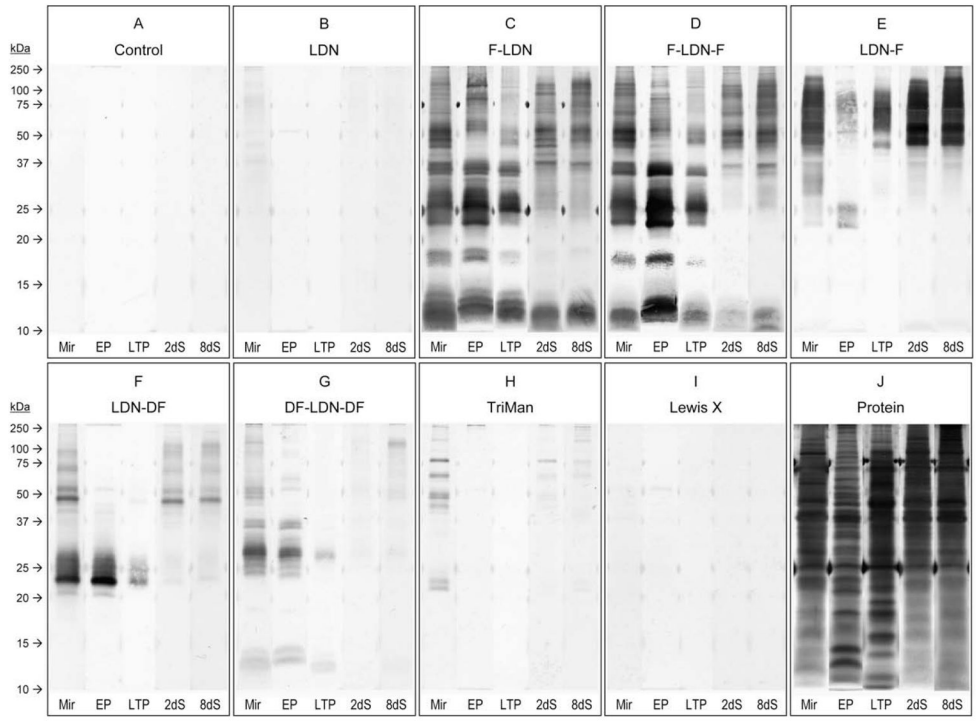

Fig. 4.

Western blots revealing glycotope expression amongst whole-body larval extracts, epidermal plate glycoproteins and parasite culture supernatants containing larval transformation proteins. Whole-body extracts of miracidia (Mir) and primary sporocysts cultivated 2 and 8 days (2dS and 8dS, respectively), as well as ciliated epidermal plate extracts (EP) and parasite culture supernatants containing larval transformation proteins (LTP), were SDS–PAGE-fractionated and immunoblotted using anti-glycotope monoclonal antibodies that recognise GalNAcβ1-4GlcNAc (LDN; (B)), Fucα1-3GalNAcβ1-4GlcNAc (F-LDN; (C)), Fucα1-3GalNAcβ1-4(Fucα1-3)GlcNAc (F-LDN-F; (D)), GalNAcβ1-4(Fucα1-3)GlcNAc (LDN-F; (E)), GalNAcβ1-4(Fucα1-2Fucα1-3)GlcNAc (LDN-DF; (F)), Fucα1-2Fucα1-3GalNAcβ1-4(Fucα1-2Fucα1-3)GlcNAc (DF-LDN-DF; (G)), Manα1-3(Manα1-6)Manβ1-4GlcNAcβ1-4GlcNAcβ1-Asn (TriMan; (H)) and Galβ1-4(Fucα1-3)GlcNAc (Lewis X; (I)). Control blots were exposed to the secondary antibody without previous primary antibody incubation (A), and total protein was visualised in-gel by silver stain (J).

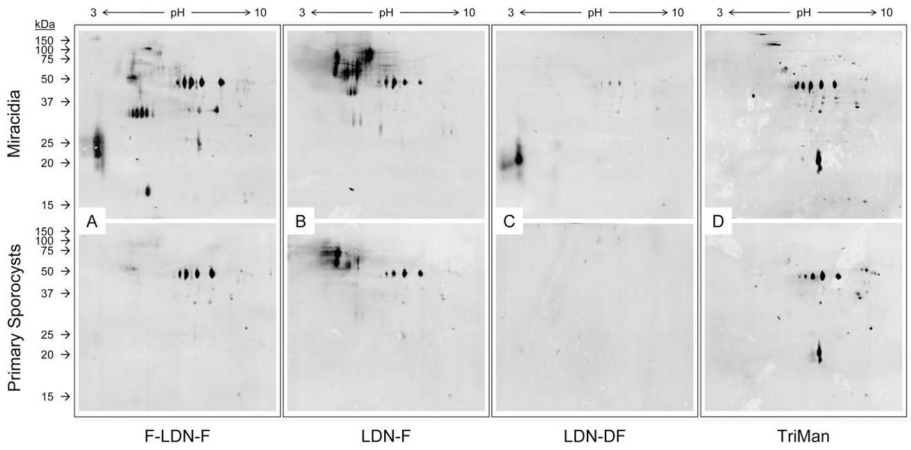

Fig. 5.

Two-dimensional (2D) Western blots demonstrating glycotope expression in surface-enriched protein extracts of miracidia and primary sporocysts. Gentle extraction of miracidia and 2-day in vitro-cultivated primary sporocysts yielded surface-enriched protein extracts that were subsequently 2D PAGE-fractionated and immunoblotted using anti-glycotope monoclonal antibodies. Panels include representative blot patterns for Fucα1-3GalNAcβ1-4(Fucα1-3)GlcNAc (F-LDN-F; (A)), GalNAcβ1-4(Fucα1- 3)GlcNAc (LDN-F; (B)), GalNAcβ1-4(Fucα1-2Fucα1-3)GlcNAc (LDN-DF; (C)) and Manα1-3(Manα1-6)Manβ1-4GlcNAcβ1-4GlcNAcβ1-Asn (TriMan; (D)).

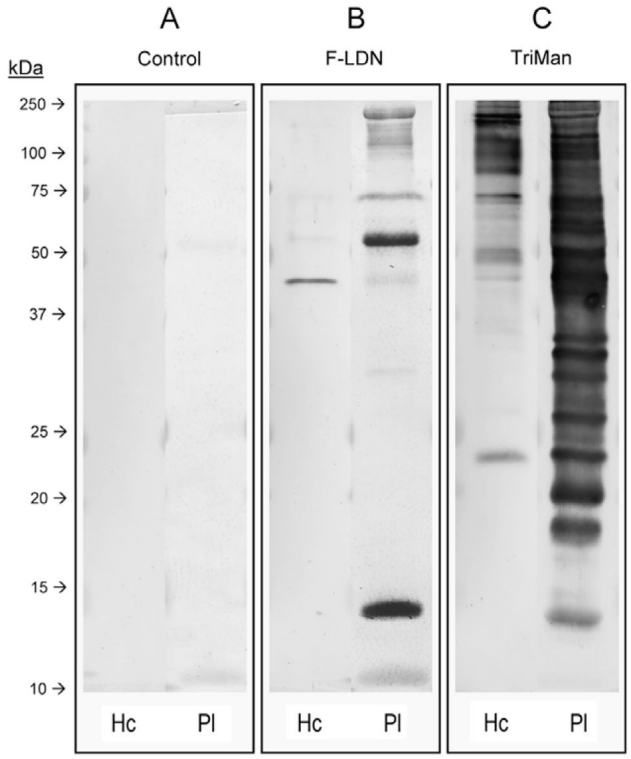

Fig. 6.

Western blot analysis of *Biomphalaria glabrata* hemocyte and plasma glycoproteins. Hemocyte (Hc) and plasma (Pl) glycoproteins of uninfected *B. glabrata* were PAGE-fractionated and immunoblotted using anti-glycotope monoclonal antibodies against Fucα1-3GalNAcβ1-4GlcNAc (F-LDN; (B)) and Manα1-3(Manα1-6)Manβ1-4GlcNAcβ1-4GlcNAcβ1-Asn (TriMan; (C)). Control blots were exposed to the secondary antibody without previous primary antibody treatment (A).

Table 1

Summary of monoclonal antibodies employed in this study and their glycotope specificities.

Monoclonal antibody	Specificity	Glycotope structure	Structure in symbols[a]	Antibody references
259-2A1	LDN	GalNAcβ1-4GlcNAcβ1-		van Remoortere et al. (2000)
258-3E3-A	F-LDN	Fucα1-3GalNAcβ1-4GlcNAcβ1-	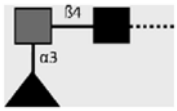	van Roon et al. (2005); C.H. Hokke, A. van Remoortere, H.J. Vermeer, A.M. Deelder (unpublished observations)
128-1E7-C	F-LDN-F	Fucα1-3GalNAcβ1-4(Fucα1-3)GlcNAcβ1-	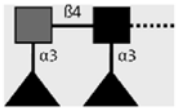	van Roon et al. (2005); C.H. Hokke, A. van Remoortere, H.J. Vermeer, A.M. Deelder (unpublished observations)
114-4E8-A	LDN-F	GalNAcβ1-4(Fucα1-3)GlcNAcβ1-	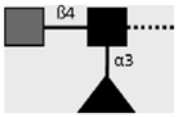	C.H. Hokke, A. van Remoortere, H.J. Vermeer, A.M. Deelder (unpublished observations)
114-5B1-A	LDN-DF	GalNAcβ1-4(Fucα1-2Fucα1- 3)GlcNAcβ1-	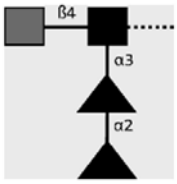	van Remoortere et al. (2000) and van Roon et al. (2005)
114-4D12-A	DF-LDN- DF	Fucα1-2Fucα1-3GalNAcβ1-4(Fucα1- 2Fucα1-3)GlcNAcβ1-	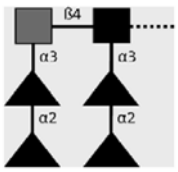	Robijn et al. (2007)
128-4F9-A	Lewis X	Galβ1-4(Fucα1-3)GlcNAcβ1-	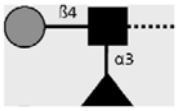	van Remoortere et al. (2000)
100-4G11-A	TriMan	Manα1-3(Manα1-6)Manβ1- 4GlcNAcβ1-4GlcNAcβ1-Asn	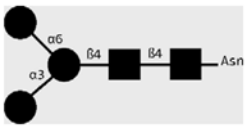	van Remoortere et al. (2003)

(▲) Fucose (Fuc), (●) Galactose (Gal), (●) Mannose (Man), (■) N-Acetylglucosamine (GlcNAc), (■) N-Acetylgalactosamine (GalNAc).

[a] Monosaccharide symbols as adopted by the Consortium for Functional Glycomics (CFG, http://functionalglycomics.org/static/consortium/).